J. Mater. Environ. Sci. 4 (5) (2013) 691-700
ISSN: 2028-2508
CODEN: JMESCN



# Substituted amines as corrosion inhibitors for N80 steel in 15%HCl

**M. Yadav *[1], Sumit Kumar [1], Usha Sharma [1], P.N. Yadav [2]**
[1]*Department of Applied Chemistry, Indian School of Mines, Dhanbad-826004,India*
[2]*Department of Physics, Post Graduate College Ghazipur, India*

Received 15 Oct 2012, Revised 14 May 2013, Accepted 14 May 2013
* Corresponding author. Email: yadav_drmahendra@yahoo.co.in

## Abstract
In the present investigation effect of Triethylenetetramine (TETA] and 2-(2-aminoethylamino) ethanol [AEAE] as corrosion inhibitors for N80 steel in 15% HCl solution was studied by polarization, AC impedance (EIS) and weight loss measurements. It was found that both the inhibitors were effective inhibitors and their inhibition efficiency was significantly increased with increasing concentration of inhibitors. Polarization studies revealed that the studied inhibitors represent mixed-type inhibitors. AC impedance studies revealed that charge transfer resistance increases and double layer capacitance decreases in presence of inhibitors. Adsorption of inhibitors at the surface of N80 steel was found to obey Langmuir isotherm.

*Keywords*: N80 steel; Corrosion inhibition; Polarization; AC impedance

## 1. Introduction
N80 steel is widely used as a construction material for pipe work in the oil and gas production, such as down hole tubular, flow lines and transmission pipelines in petroleum industry. Acid solutions are extensively used in a variety of industrial processes such as oil well acidizing, acid pickling and acidic cleaning [1], which generally lead to serious metallic corrosion. Corrosion inhibitors are widely used in stimulation operations in petroleum wells [2, 3]. In these operations acid solutions at temperatures up to 333 K are often employed to remove iron oxides and carbonated minerals. In such aggressive medium, the use of corrosion inhibitors is one of the most common, effective and economic methods to protect metals in acid media [4]. The majority of the well-known inhibitors are organic compounds containing heteroatoms such as oxygen, nitrogen or sulfur, and multiple bonds, which allow an adsorption on the metal surface [5, 6]. It has been observed that the adsorption of these inhibitors depends on the physio-chemical properties of the functional groups and the electron density at the donor atom. The adsorption occurs due to the interaction of the lone pair and/or π-orbitals of inhibitor with d-orbitals of the metal surface atoms, which evokes a greater adsorption of the inhibitor molecules onto the surface, leading to the formation of a corrosion protection film [7]. Furthermore, adsorption is also influenced by the structure and the charge of metal surface, and the type of testing electrolyte [8]. The choice of effective inhibitors is based on their mechanism of action and electron-donating ability. The significant criteria involved in this selection are molecular structure, electron density on the donor atoms, solubility and dispersibility [9]. Aliphatic amines, heterocyclic amines, and aromatic amines have been investigated as corrosion inhibitors [10,11]. Derivatives of amines [12-15] have also been reported as good corrosion inhibitors for metals in different acid solution.
The purpose of this study is to evaluate the protective ability of Triethylenetetramine (TETA] and 2-(2-aminoethylamino) ethanol [AEAE] as corrosion inhibitors for N80 steel in 15% hydrochloric acid.

## 2. Material and Methods
### *2.1. Materials*
The corrosion tests were performed on N80 steel samples with a composition (wt. %): C: 0.31, Mn: 0.92, Si: 0.19, P: 0.01, S: 0.008, Cr: 0.20, Fe: Remainder. Mild Steel coupons having dimension 3.0 cm × 3.0 cm × 0.1 cm size were mechanically cut and for the surface finish coupons were abraded with different grade emery papers (120, 220, 400, 600, 800, 1500 and 2000 grade) for weight loss experiment. For Electrochemical measurements mild steel coupons having dimension 1.0 cm × 1.0 cm × 0.1 cm were mechanically cut and abraded with same manner as before, with an

exposed area of 1 $cm^2$ (rest covered with araldite resin) with 3 cm long stem. Prior to the experiment specimens were washed with distilled water, degreased in acetone and dried at room temperature.
The studied inhibitors triethylenetetramine (TETA] and 2-(2-aminoethylamino) ethanol [AEAE] were purchased from Merk.The structure of the inhibitors is given below:

$[H_2N\text{-}(CH_2)_2\text{-}NH\text{-}(CH_2)_2\text{-}NH\text{-}(CH_2)_2\text{-}NH_2]$ (TETA)

$[OH\text{-}(CH_2)_2\text{-}NH\text{-}(CH_2)_2\text{-}NH_2]$ (AEAE)

*2.2 Weight loss measurements*
The specimens for the weight loss measurements were of the size 3cm × 3cm × .1cm. For weight loss experiments 300 mL of 15% HCl (v/v) was taken in 500 mL glass beakers. The inhibition efficiencies (IE) were evaluated after a pre-optimized time interval of 6 h using 50, 100, 200, 300 and 500 ppm by weight of inhibitors. The specimens were removed from the electrolyte, washed thoroughly with distilled water, dried and weighed. The inhibition efficiencies (IE) were calculated using the equation:

$$\%IE = [(CR_0\text{-}CR_i) / CR_0] \times 100 \quad (1)$$

where $CR_0$ is the weight loss in absence of inhibitor and $CR_i$ is the weight loss in presence of inhibitor.
Corrosion rate (CR) for the specimen was calculated with the help of the equation

$$CR\ (mpy) = \frac{534W}{DAT} \quad (2)$$

where, W = weight loss (mg)
D = Density of specimen ($g/cm^3$)
A = Area of specimen ($cm^2$)
T = Exposure time (hours)
Influence of temperature (298 to 333 K) on the inhibition behavior was studied by repeating the weight loss measurements at each temperature and calculating the values of rate of corrosion, inhibition efficiencies and activation and thermodynamic parameters.

*2.3 Electrochemical Polarization Studies*
The electrochemical studies were performed in a three necked glass assembly containing 150 mL of the electrolyte with different concentrations of inhibitors (from 50 ppm to 500 ppm by weight) dissolved in it. The potentiodynamic polarization studies were carried out with N80 steel electrode having an exposed area of $1cm^2$. A conventional three electrode cell consisting of N80 steel as working electrode, platinum as counter electrode and a saturated calomel electrode as reference electrode were used. Polarisation studies were carried out using VoltaLab 10 electrochemical analyzer and data was analysed using Voltamaster 4.0 software. The potential sweep rate was 1 $mVs^{-1}$. All experiments were performed at 25 ± 0.2°C in an electronically controlled air thermostat. For calculating inhibition efficiency by electrochemical polarization method, the following formula was used:

$$\%IE = [(I_0 - I_{inh}) / I_0] \times 100 \quad (3)$$

where, $I_0$ is corrosion current in absence of inhibitor and $I_{inh}$ is the corrosion current in presence of inhibitor.

*2.4. AC Impedance Studies*
AC impedance studies were carried out in a three electrode cell assembly using computer controlled VoltaLab 10 electrochemical analyzer, as well as N80 steel as the working electrode, platinum as counter electrode and saturated calomel as reference electrode.The data were analyzed using Voltamaster 4.0 software. The electrochemical impedance spectra (EIS) were taken in the frequency range from 10 kHz to 1mHz at the rest potential by applying 5mV sine wave AC voltage. The charge transfer resistance ($R_{ct}$ ) and double layer capacitance ($C_{dl}$) were determined from Nyquist plots. The inhibition efficiencies were calculated from charge transfer resistance values by using the equation

$$\%IE = [ (R_{ct(inh)} - R_{ct}) / R_{ct(inh)}] \times 100 \quad (4)$$

where $R_{ct}$ is the charge transfer resistance in absence of inhibitor and $R_{ct(inh)}$ is the charge transfer resistance in presence of inhibitor.

*2.5. Scanning electron microscopic (SEM) analysis*
In order to observe the changes in surface morphologies of corrosive samples before and after the addition of inhibitor, the N80 steel specimens were immersed in 15% HCl solutions in the absence and presence of optimum concentration

of inhibitor for 6 h at 25 ºC. After immersion for 6 h the specimens were taken out from the solution and cleaned with distilled water, dried using a cold air blaster, and then the surface was investigated by a JSM-5800, MODEL S-3400N scanning electron microscope (SEM).

## 3. Results and Discussion

*3.1 Weight loss study*

Weight loss studies were performed in accordance with ASTM method. Tests were conducted in 15% HCl (v/v) solution for without and with different concentration of inhibitors (50-500 ppm) at different temperatures (298 to 333 K).

*3.1.1 Effect of concentration*

Both the inhibitors were tested for 6h exposure period at different concentrations and their corresponding weight loss data are presented in Table 1. The inhibitors TETA and AEAE show corrosion inhibition efficiency of 89.2% and 80.2% respectively (Table.1) at 500 ppm concentration. The corrosion rate decreases with an increase in concentration of each inhibitor (Figure 1), indicating that adsorption of inhibitors increases as concentration increases, resulting in reduction of corrosion rate.

*3.1.2 Effect of temperature*

The effect of temperature on the performance of TETA and AEAE as corrosion inhibitors for N80 steel in 15% HCl was investigated by weight loss measurements in the temperature range 298-333 K in absence and presence of optimum concentration (500 ppm) of inhibitors. The variation of inhibition efficiency and corrosion rate with temperature is shown in Table 2. The observation depicts that rate of corrosion increases and no pitting was observed with increase in temperature. This may be due to the fact that at higher temperature the metal organic complex layer dissociates leaving a porous diffused film, which is responsible for corrosion [16].

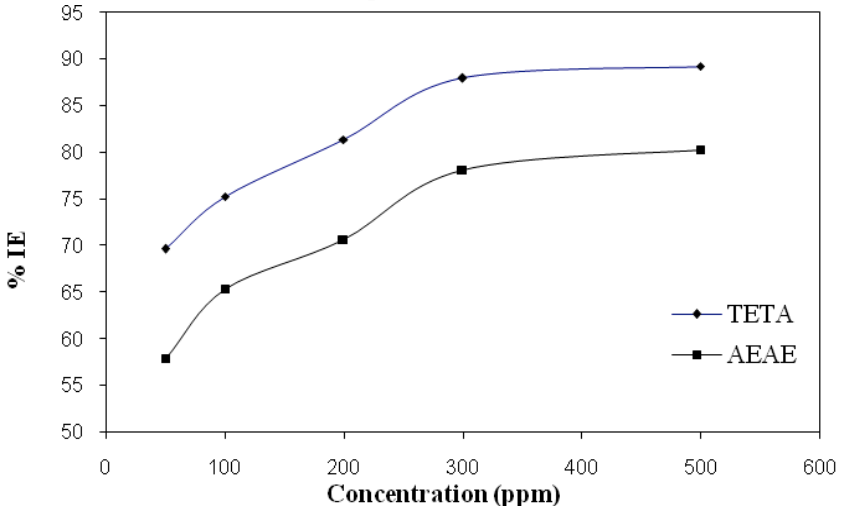


**Figure 1**: Variation of inhibition efficiency with concentration in presence of TETA and AEAE.

**Table 1:** Corrosion inhibition of N80 steel in 15% HCl in presence and absence of inhibitors TETA and AEAE at different concentration

| Conc. (ppm) | TETA | | AEAE | |
|---|---|---|---|---|
| | CR (mpy) | %IE | CR (mpy) | %IE |
| 0 | 9.55 | - | 9.55 | - |
| 50 | 2.9 | 69.6 | 4.0 | 57.9 |
| 100 | 2.4 | 75.2 | 3.3 | 65.3 |
| 200 | 1.8 | 81.3 | 2.8 | 69.6 |
| 300 | 1.1 | 87.9 | 2.1 | 78.1 |
| 500 | 1.0 | 89.2 | 1.9 | 80.2 |

**Table.2:** Corrosion parameters in absence and in presence of optimum concentration of TETA and AEAE at different temperatures.

| Temperature (K) | Blank | | TETA | | AEAE | |
|---|---|---|---|---|---|---|
| | CR (mpy) | %IE | CR (mpy) | %IE | CR (mpy) | %IE |
| 298 | 9.55 | - | 1.03 | 89.2 | 1.89 | 80.2 |
| 303 | 12.09 | - | 1.91 | 84.2 | 2.77 | 77.1 |
| 313 | 19.27 | - | 3.84 | 80.1 | 4.82 | 75.0 |
| 323 | 30.42 | - | 7.88 | 74.1 | 9.47 | 68.9 |
| 333 | 48.94 | - | 15.80 | 67.7 | 18.26 | 62.7 |

*3.1.3 Adsorption Isotherms*

To determine the adsorption mode, various isotherm were tested and Langmuir adsorption isotherms was found to be best, which gives a straight line graph for the plot of log ( θ/1-θ ) verses logarithmic concentration (M) of inhibitors (Figure 2). The surface coverage data of TETA and AEAE shows that both the inhibitors followed Langmuir adsorption isotherm indicating that adsorption is the root cause of corrosion inhibition. The correlation coefficients ($R^2$) values of both studied inhibitors in presence of inhibitors at 25˚C are near to unity, while slope values are 0.999, and 0.998 for TETA and AEAE respectively, suggesting that the Langmuir adsorption isotherm fits best with the experimental data.

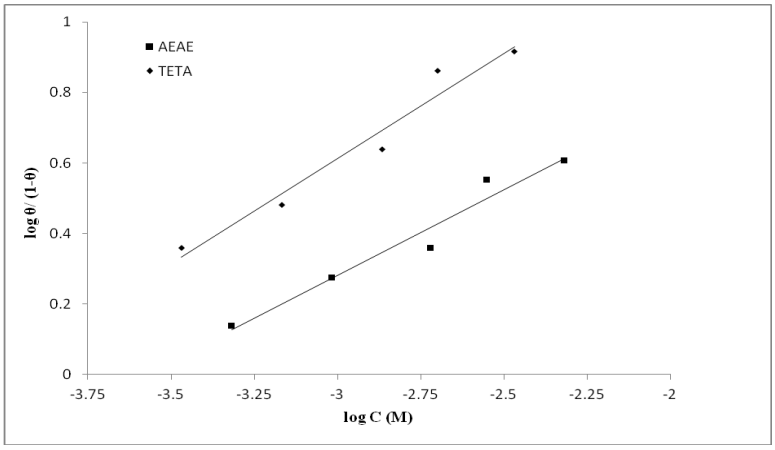


**Figure 2.** Langmuir plots for TETA and AEAE.

The inhibition efficiency afforded by TETA and AEAE may be attributed to the presence of electron rich N atoms of $–NH_2$ group. In the aqueous acidic solutions TETA and AEAE exist either as neutral molecules or in the form of protonated molecules (cations). These inhibitors may adsorb on the metal/acid solution interface by one and/or more of the following ways:

(i) electrostatic interaction of protonated inhibitors with already adsorbed chloride ions,
(ii) interaction between unshared electron pairs of hetero-atoms and vacant d orbital of iron surface atoms.

Generally, two modes of adsorption could be considered. In one mode, the neutral inhibitors may be adsorbed on the surface of N80 steel through the chemisorptions mechanism, involving the displacement of water molecules from the N80 steel surface and the sharing electrons between the hetero-atoms and iron. In another mode, since it is well known that the steel surface bears positive charge in acid solution [17], so it is difficult for the protonated inhibitors to approach the positively charged mild steel surface ($H_3O^+$/metal interface) due to the electrostatic repulsion. Since chloride ions have a smaller degree of hydration, thus they could bring excess negative charges in the vicinity of the interface and favour more adsorption of the positively charged inhibitor molecules, the protonated inhibitors adsorb through electrostatic interactions between the positively charged molecules and the negatively charged metal surface. Thus there is a synergism between adsorbed $Cl^-$ ions and protonated inhibitors. Experimental data reveals that % IE inhibitors are in the order TETA>AEAE.

*3.1.4 Kinetic and thermodynamic study*

The apparent activation energy ($E_a$) was calculated by using Arrhenius equation:

$$\log k = - E_a /2.303RT + \log A \quad (5)$$

where, k is rate of corrosion, $E_a$ is the apparent activation energy, R is the universal gas constant, T is absolute temperature and A is the Arrhenius pre exponential factor. By plotting log k against 1/T the values of activation energy ($E_a$) has been calculated ($E_a$ = - (Slope) × 2.303 × R) (Figure 3). Activation energy for N80 steel in 15% HCl increases in presence of inhibitors. It is evident from Table 3 that, the values of $E_a$ were higher for inhibited solutions as compared to the uninhibited solutions indicating that the energy barrier for the corrosion reaction increases due to physical adsorption of the inhibitors on the metal surface.

The values of entropy of activation (ΔS*) and enthalpy of activation (ΔH*) were calculated by using the equation

$$k = (RT/Nh) \exp(\Delta S^*/R) \exp(-\Delta H^*/RT) \quad (6)$$

where k is rate of corrosion, h is Planks constant, and N is Avogadro′ s number. A plot of log ( k/T) verses 1/T (Figure 4) gives a straight line, with a slope of (-ΔH*/2.303R) and a intercept of [log (R/N h) + ΔS*/2.303R], from which the values of ΔS* and ΔH* were calculated (Table 3).The $\Delta H^*$ values for TETA and AEAE were found to be as -35.7 kJ/mol and -38.2 kJ/mol respectively, revealed the exothermic nature of corrosion reaction. The $\Delta S^*$ values were found to be -65.4 J/mol, and -81.1 J/mol for TETA and AEAE respectively (Table 3). The negative values of ΔS* obtained in the inhibited and uninhibited solutions suggest that the activated complex is the stage that determines the corrosion rate [18].The negative values of the entropy change of activation (ΔS*) for TETA and AEAE also imply that the activated complex in the rate determining step represents an association rather than a dissociation step, indicating that a decrease in disordering takes place on going from reactants to the activated complex [19].

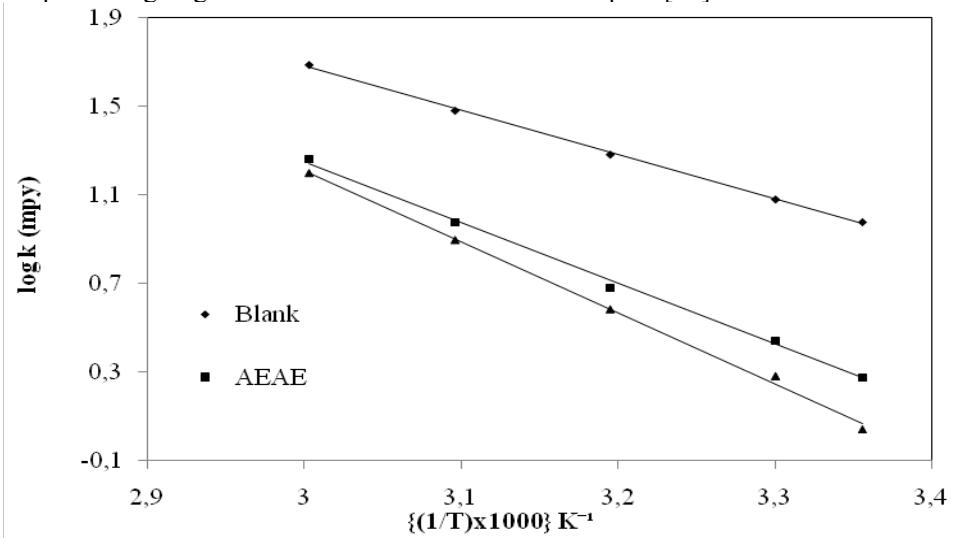


**Figure 3:** Arrhenius plot for the corrosion of N80 steel in 15%HCI in presence of 500 ppm of TETA and AEAE.

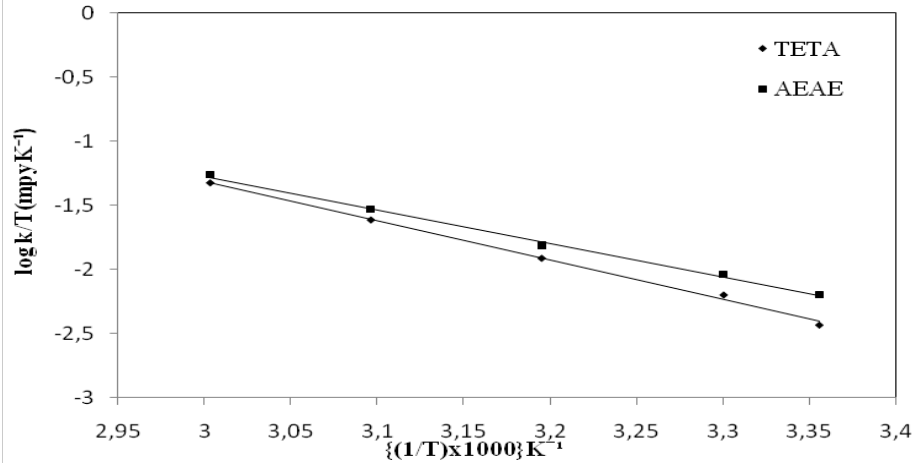


**Figure 4:** A plot of log k/T vs 1/T in presence of 500 ppm of TETA and AEAE.

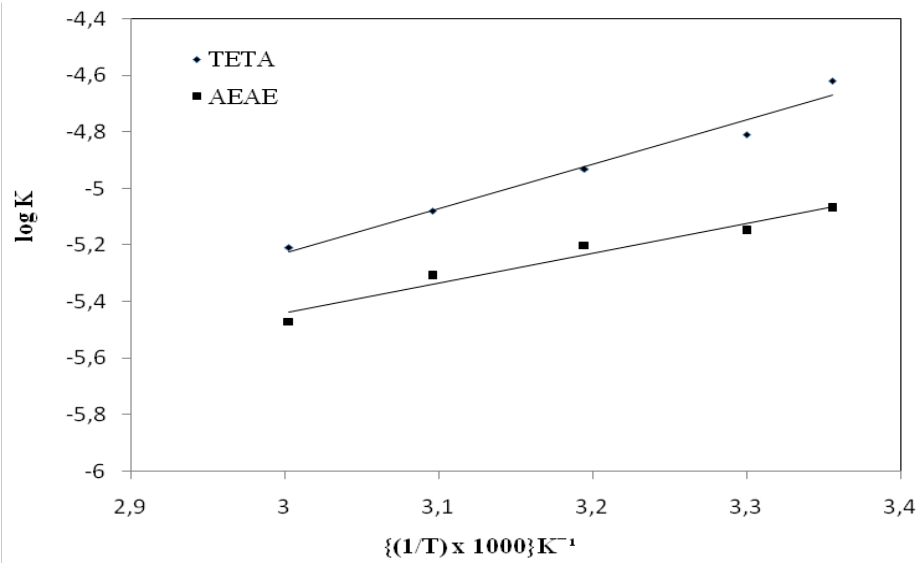


**Figure 5:** A plot of log K vs 1/T in presence of 500 ppm of TETA and AEAE.

The average value for free energy of adsorption ($\Delta G_{ads}$), were calculated using the equation:

$$K = \frac{1}{55.5}\exp\left(\frac{-\Delta Gads}{RT}\right) \quad (7)$$

where R is molar gas constant in and T is temperature. The value of 55.5 in the above equation is the concentration of water in the solution in mole/liter. The equilibrium constant (K) has been replaced by the equation

$$K = \theta/(1-\theta)C \quad (8)$$

where θ is degree of coverage on metal surface, C is concentration of inhibitors in moles/liter.

**Table 3:** Thermodynamic parameter in absence and in presence of TETA and AEAE

| Inhibitor | $\Delta H^*$ (kJ mol$^{-1}$) | $E_a$ (kJ mol$^{-1}$) | $\Delta G_{ads}$ (kJ mol$^{-1)}$ | $\Delta S^*$ (J mol$^{-1}$ K$^{-1}$) |
|---|---|---|---|---|
| Blank | - | 38.4 | - | - |
| TETA | -45.7 | 56.6 | -37.6 | -65.4 |
| AEAE | -48.2 | 48.5 | -32.7 | -81.1 |

By plotting log K against 1/T the values of $\Delta G_{ads}$ were calculated ($\Delta G_{ads}$ = - 2.303× R × Slope) (Figure 5). The values of free energy of adsorption ($\Delta G_{ads}$) for TETA and AEAE were found to be -37.6 kJ/mol and -32.7 kJ/mol respectively (Table 3). Values of $\Delta G_{ads}$ around -20 kJ /mol or lower are consistent with the electrostatic interaction between charged organic molecules and the charged metal surface (physisorption); those around -40 kJ/ mol or higher involve charge sharing or transfer from the organic molecules to the metal surface to form a co-ordinate type of bond (chemisorptions). The values of $\Delta G_{ads}$ for TETA and AEAE was found to be -37.6 kJ/mol and -32.7 kJ/mol which is less than -40 kJ /mol indicated that in addition to electrostatic interaction, there may be some other interactions [20]. Lebrini et al. [21] studied some triazole derivatives as corrosion inhibitors for mild steel in 1 M $HClO_4$. They reported that the Gibbs free energy of adsorption of these molecules were around -34 kJ /mol. They concluded that the adsorption mechanism of these molecules on steel involved two types of interactions, chemisorptions and physisorption. Similar conclusion was found by Ozcan [22], who studied the use of cystine as a corrosion inhibitor on mild steel in sulfuric acid. Thus, adsorption of studied inhibitors at the surface of N80 steel is not pure physisorption but it is combination of physisorption as well as chemisorptions.

*3.2. Potentiodynamic polarization study*

Figures 6 and 7 show the polarization curves of N80 steel in15% HCl solution in absence and presence of 50,200 and 500 ppm of inhibitors TETA and AEAE respectively.

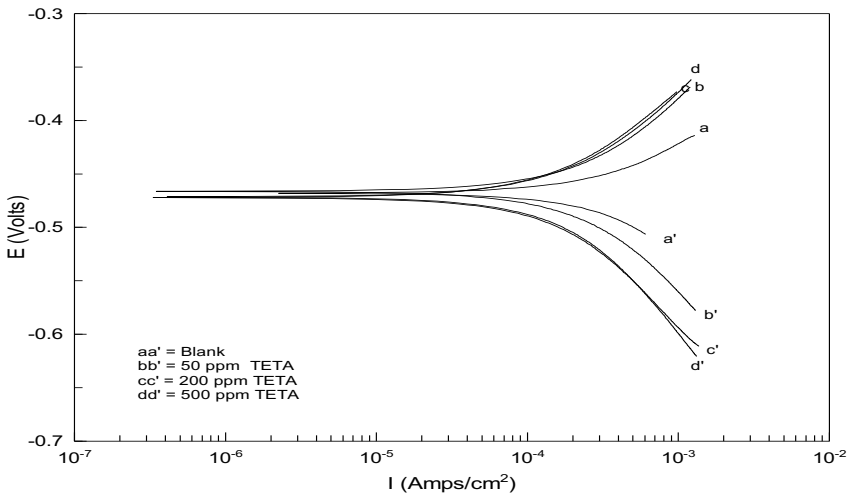


**Figure 6:** Potentiodynamic polarization curves for N80 Steel in 15% HCl in absence and in presence of TETA.

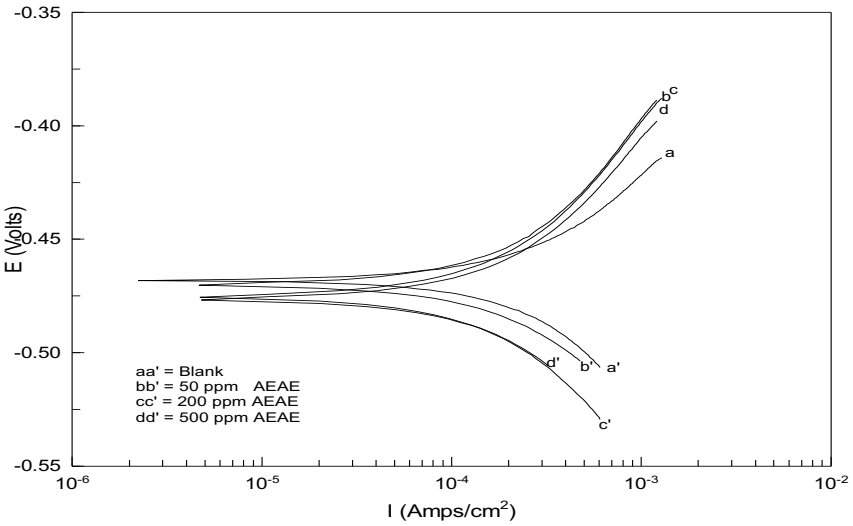


**Figure 7:** Potentiodynamic polarization curves for N80 Steel in 15% HCl in absence and in presence of AEAE.

The nature of the polarization curves remains almost same in absence and presence of both the inhibitors but in presence of inhibitors the curves shifted towards the lower current density as compared to the blank. The shift in current density towards lower current density in presence of inhibitors increases on increasing the concentration of the inhibitors. The electrochemical corrosion parameters including corrosion current densities ($I_{corr}$), corrosion potential ($E_{corr}$), cathodic Tafel slope ($\beta_c$), anodic Tafel slope ($\beta_a$), and inhibition efficiency obtained from the polarization curves of TETA and AEAE are presented in Table 4. It is clear from the Figures 6 & 7 that with the increase of inhibitors concentration both anodic and cathodic currents were inhibited. It is apparent from the Table 4 that $I_{corr}$ decreases considerably in the presence of both the inhibitors, and %IE increases with the increase in the inhibitor concentration, due to the increase in the blocked fraction of the metal surface by adsorption. The value of anodic and cathodic Tafel slopes increases in presence of both the inhibitors as compared to the blank solution. A minor shift in $E_{corr}$ values towards the negative direction was obtained in presence of both the inhibitors, indicating mixed nature of the

inhibitors. Generally, if the displacement in $E_{corr}$ is >85 mV with respect to $E_{corr}$ in uninhibited solution, the inhibitor can be seen as a cathodic or anodic type [23, 24]**.** In our study the maximum displacement is 4 mV in TETA and 3 mV in AEAE, which indicates that both inhibitors can be arranged as a mixed type inhibitor.

**Table 4:** Electrochemical corrosion parameters in absence and in presence of TETA and AEAE at different concentrations

| Inhibitors | Conc . (ppm) | Tafel slopes | | $I_{corr}$ ($\mu A/cm^2$) | $E_{corr}$ (mV) | %IE | %IE from wt. loss |
|---|---|---|---|---|---|---|---|
| | | $\beta_a$ ($mVdec^{-1}$) | $\beta_c$ ($mVdec^{-1}$) | | | | |
| Blank | - | 109 | 153 | 471 | -468 | - | - |
| TETA | 50 | 113 | 165 | 141 | -471 | 70.1 | 69.6 |
| | 200 | 116 | 178 | 86 | -467 | 81.7 | 79.2 |
| | 500 | 122 | 185 | 42 | -472 | 91.1 | 89.2 |
| AEAE | 50 | 111 | 166 | 182 | -469 | 61.4 | 57.9 |
| | 200 | 115 | 172 | 141 | -468 | 70.1 | 70.6 |
| | 500 | 120 | 179 | 95 | -471 | 79.8 | 80.2 |

*3.3. Electrochemical impedance spectroscopy*

Nyquist plots of N80 steel in 15% HCl in the presence and absence of different concentrations (50,200 and 500 ppm) of TETA and AEAE at 25±1°C are shown in the Figures 8 & 9. All the impedance diagrams were analyzed in terms of the equivalent circuit which is a parallel combination of the charge transfer resistance ($R_{ct}$) and the constant phase element of double layer (CPE), both in series with the solution resistance ($R_s$). CPE is mathematically expressed as:

$Z_{CPE} = Y_0^{-1}(i\omega)^{-n}$

where $Y_0$ is a proportionality factor and 'n' has the meaning of phase shift. The value of n represents the deviation from the ideal behavior and it lies between 0 and 1.

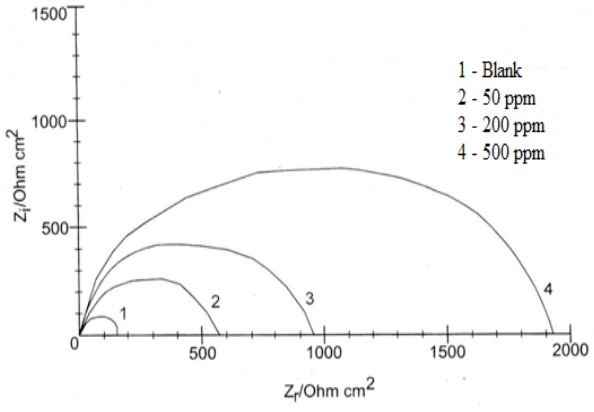


**Figure 8:** Nyquist plots of the corrosion of N80 steel in 15% HCl at different concentrations of TETA.

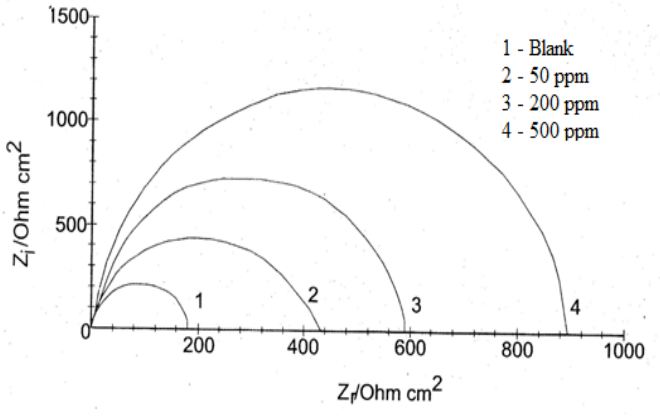


**Figure 9:** Nyquist plots of the corrosion of N80 steel in 15% HCl without and with different concentrations of AEAE

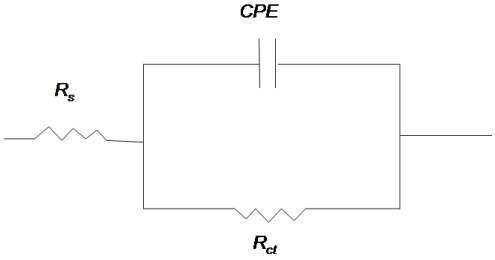


**Figure 10:** Equivalent circuit diagram.

**Table 5:** Electrochemical impedance parameters in absence and in presence of TETA and AEAE

| Inhibitors | Conc. (ppm) | $R_{ct}$ ($\Omega cm^2$) | $C_{dl}$ ($\mu F\ cm^{-2}$) | IE% |
|---|---|---|---|---|
| Blank | - | 176 | 362 | - |
| TETA | 50 | 598 | 179 | 70.6 |
| | 200 | 935 | 158 | 81.2 |
| | 500 | 1914 | 94 | 90.8 |
| AEAE | 50 | 423 | 160 | 58.5 |
| | 200 | 564 | 125 | 68.8 |
| | 500 | 881 | 90 | 80.0 |

All the Nyquist plots obtained were semicircle in nature and the diameter of the semicircles were increases with increase in inhibitor concentration and shape is maintained throughout the tested concentration, indicating that almost no change in the corrosion mechanism occurs due to inhibitor action. The electrochemical parameters ($R_{ct}$, $C_{dl}$) calculated from the Nyquist plots (Figure 10) in presence and absence of inhibitors are presented in Table 5. The values of electrochemical double layer capacitance ($C_{dl}$) were calculated at the frequency $f_{max}$, at which the imaginary component of the impedance is maximal ($-Z_i$) by the equation:

$$C_{dl}=1/2\pi f_{max}R_{ct} \quad (8)$$

In EIS study an increase in $R_{ct}$ value is observed with increasing the inhibitors concentration, suggesting that the charge transfer process is retarded due to decrease in the uncovered surface available for corrosion reaction. Due to the nonhomogeneity or roughness of the metal surface the observed semicircles of capacitive loops was depressed into the Zi which is often referred to as frequency dispersion [25]. It is worth mentioning that the double layer capacitance ($C_{dl}$) value is affected by imperfections of the surface. The $C_{dl}$ values found to decrease with increase in concentration of inhibitors solutions. This behavior is generally seen for system where inhibition occurred due to the formation of a surface film by the adsorption of inhibitor on the metal surface [26]. Decrease in $C_{dl}$, which can result from a decrease in local dielectric constant and/or an increase in the thickness of the electrical double layer, suggest that the inhibitor molecules act by adsorption at the metal/solution interface [27].

*3.4. SEM study of metal surface product*

SEM microphotographs (Figure 11 A,B,C,D) of the film formed on the metal surface at 1000X magnifications were studied to analyze the change in the morphology of the metal surface after corrosion tests in presence and absence of the inhibitors.

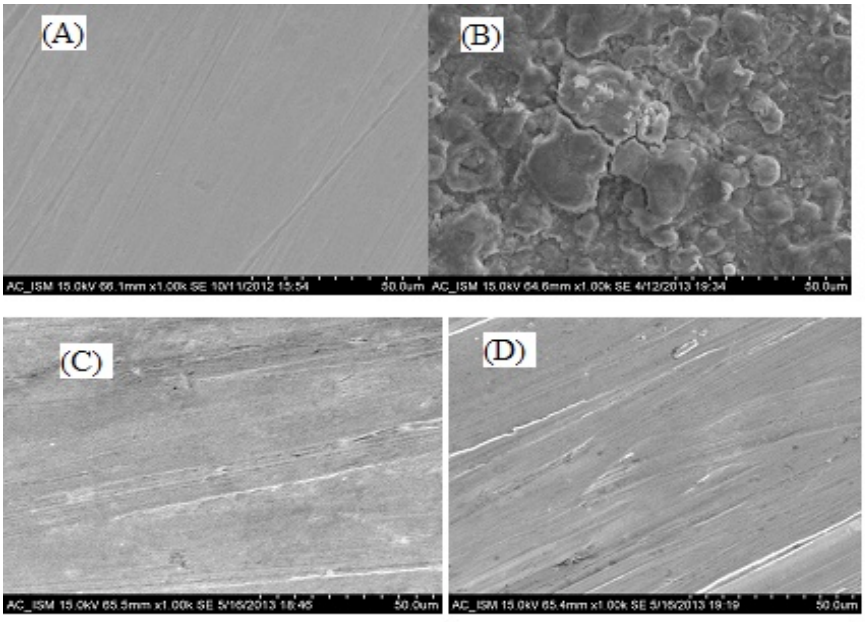


**Figure 11 :** SEM of (A) Polished sample (B) Sample in presence of 15% Hydrochloric acid (C) Sample in presence of 500 ppm of TETA (D) Sample in presence of 500 ppm of AEAE.

Figure 11 (A) shows the SEM of polished sample (magnification 1000X). Fig. 11(B) shows the SEM microphotographs of N80 steel (magnification 1000X) when exposed to 15% HCl solution at room temperature in absence of inhibitors. Figure 11 (C, D) are the microphotographs of the metal surface when exposed to the acid medium in presence of TETA and AEAE respectively at the same magnifications. Fig 11 (B) shows that the steel surface appears to be very rough in absence of inhibitors. This is due to formation of uniform flake type corrosion products on the metal surface. No pitting and other separate phase are visible in microphotograph. Fig. 11 (C, D) are the microphotographs of the metal surface when exposed to the acid medium in presence of TETA and AEAE respectively at the same magnifications. In comparison to the microphotograph of the steel surface without inhibitor with the photographs of the exposed surface in presence of inhibitors are found to be covered with a semi globular type protective film of compounds uniformly spread over the surface. The protective film is formed due to adsorption of the inhibitor molecules on the steel surface.

## Conclusion

TETA and AEAE both act as good corrosion inhibitors for corrosion of N80 steel in 15% HCl solution. The inhibition efficiency values increases with the increase in inhibitors concentration, but decreases with increasing temperature for corrosion of N80 steel in 15% HCl. The adsorption of the TETA and AEAE on N80 steel surface obeys Langmuir adsorption isotherm. Variation in the values of $\beta_a$ and $\beta_c$ (Tafel slopes) and negative shift in the values of corrosion potential ($E_{corr}$) indicate that both the tested inhibitors are mixed type but predominantly control the cathodic reactions. EIS measurements show that charge transfer resistance ($R_{ct}$) increases and double layer capacitance($C_{dl}$) decreases in presence of inhibitors.The SEM of the inhibited metal surface suggested the adsorption of the inhibitor molecules on the surface of N80 steel.

## Acknowledgements

Financial assistance from Indian School of Mines, Dhanbad under the “Faculty Research Scheme” to M. Yadav is gratefully acknowledged.

## Reference

1. Yadav M., Sharma U., *J. Mater. Environ. Sci.* 2 (2011) 407.
2. Ajmal M., Mideen A.S. and Quraishi M.A. *Corros. Sci*., 36 (1994) 79.
3. Bethencourt M., Botana F.J., Calvino J.J. and Marcos M., *Corros. Sci.,* 40 (1998) 1803.
4. Khaled K. F., Mghraby A. E., Ibrahim O. A., Elhabib O. A. and Ibrahim M. A. M., *J. Mater. Environ. Sci.* 1 (2010) 139.
5. Bentiss F. and Lagrenée M., *J. Mater. Environ. Sci.* 2 (1) (2011) 13.
6. Nazeer Ahmed Abdel , Fouda A.S. and Ashour E.A., *J. Mater. Environ. Sci.* 2 (1) (2011) 24.
7. Benali Omar , Larabi Lahcene , Merah Salah and Harek Yahia, *J. Mater. Environ. Sci.* 2 (1) (2011) 39.
8. Obot I.B., Obi-Egbedi N.O. and Umoren S.A., *Int. J. Electrochem. Sci.*, 4 (2009) 863.
9. Obot I.B., *Port. Electrochim. Acta,* 27 (2009) 539.
10. Hackerman M. and Sudbery J.D, *J. Electrochem. Soc.,* 97 (1950) 109.
11. Patel N.K., Sampat S.S., Vora J.C. and Trivedi R.M., *Werkst. Korros.,* 10 (1970) 809.
12. Desai M.N. and Shah Y.C.: *Corros. Sci*., 12 (1972) 725.
13. Sathiyanarayanan S., Marikkannu C. and Palaniswamy N., *Appl. Surf. Sci.* 241 (2005) 477.
14. Herrag L. , Hammouti B. , Elkadiri S. , Aouniti A. , Aouniti C. Vezin H. and Bentiss F. , *Corros. Sci.,* 52 (2010) 3042.
15. Bhajiwala H.M. and Vashi R.T, Bull. Electrochem., 17 (2001) 441.
16. Putolova I.N., Balezin S.A. and Barannik:V.P., *Metallic Corrosion Inhibitors*, Pergamann Press, NY 1960.
17. Mu G.N., Zhao T.P., Liu M. and Gu T., *Corrosion,* 52 (1996) 853.
18. Al-Juaid S. S., *Chemistry and Technology of Fuels and Oils,* 47 (2011) 58.
19. Olivares O., Likhanova N.V. and Gomez B., *Appl. Surf. Sc.,* 252 (2006) 2894.
20. Behpour M., Ghoreishi S.M., Soltani N., Salavati-Niasari M., Hamadanian M., Gandomi A., *Corros. Sci*., 50 (2008) 2172
21. Lebrini,M,. Traisnel M., Lagrene M., Mernari B. and Bentiss F., *Corros. Sci*., 50 (2008) 473.
22. Ozcan M., *Journal of Solid State Electrochemistry*, 12 (2008) 1653.
23. Ashassi-Sorkhabi H., Majidi M.R. and Seyyedi K., *Appl. Surf. Sci.,* 225 (2004) 176.
24. Li X.H., Deng S.D. and Fu H.: *Corros. Sci*., 51 (20090 1344.
25. Lebrini M., Lagrenée M. and Bentiss F., *Corros. Sci*. 49 (2007) 2254.
26. Rosenfield I.L.: *Corrosion Inhibitors*, McGraw-Hill, New York, 1981.
27. MaCafferty M. and Hackerman N., *J. Electrochem. Soc*., 119 (1972) 146.